J. Fluid Mech. (1988), *vol.* 190, *pp.* 321–342
Printed in Great Britain

Steady-state coating flows inside a rotating horizontal cylinder

By R. E. JOHNSON
Department of Theoretical and Applied Mechanics, University of Illinois, Urbana, IL 61801, USA

(Received 4 June 1987 and in revised form 27 October 1987)

Thin coating flows inside a rotating circular cylinder are investigated when the axis of rotation is perpendicular to the direction of gravity. Attention is restricted to flows of power-law fluids having negligible inertia. Four distinct steady-state liquid-film profiles are found to be possible. Two of the cases correspond to a continuous coating, i.e. films that cover the entire inner surface of the cylinder. The other two cases involve partial films covering a limited portion of the cylinder surface. Of the two continuous films, one is the expected configuration involving a coating that gradually changes in thickness as one moves around the cylinder, the film being thicker on the ascending portion of the cylinder and thinner on the descending portion. The second continuous-film configuration has regions on the rising side of cylinder where a rapid change in depth is possible. This case also has the potential to have recirculating zones where a portion of the fluid is trapped in either one or two eddies at fixed locations on the rising side of the cylinder. Of the two partial films, one corresponds to a weakly deformed puddle at the bottom of the cylinder and is the appropriate solution at small rotation rates. The second partial film is a film which coats a portion of the ascending side of the cylinder, the extent of which depends on the film volume.

1. Introduction

Steady-state coating flows inside a rotating horizontal drum are considered. Coating flows are among an important class of flows commonly found in manufacturing. The case considered here is of particular interest in rotational moulding, some pipe-coating processes and in the manufacture of pipes and columns from molten metals and cements. The special case of a continuous coating inside a rotating circular cylinder, sometimes referred to as a rimming flow, has been studied by Ruschak & Scriven (1976), Deiber & Cerro (1976) and Orr & Scriven (1978). In addition to restricting their attention to the case when the coating completely covers the inner surface of the cylinder, each of these papers also restrict attention to Newtonian fluids. Ruschak & Scriven consider the limiting case when the motion of the liquid is a small perturbation from a rigid-body motion and they consider both large and small Reynolds-number limits of their solution. Deiber & Cerro solve the corresponding boundary-layer equations numerically using a streamline coordinate system, and Orr & Scriven present results from a finite-element numerical simulation of the rimming flow including surface-tension effects. Deiber & Cerro speculated on the existence of discontinuous solutions when their numerical scheme failed to converge. The present paper, for the first time, clearly identifies some of these discontinuous solutions. Deiber & Cerro also briefly considered the low-Reynolds-

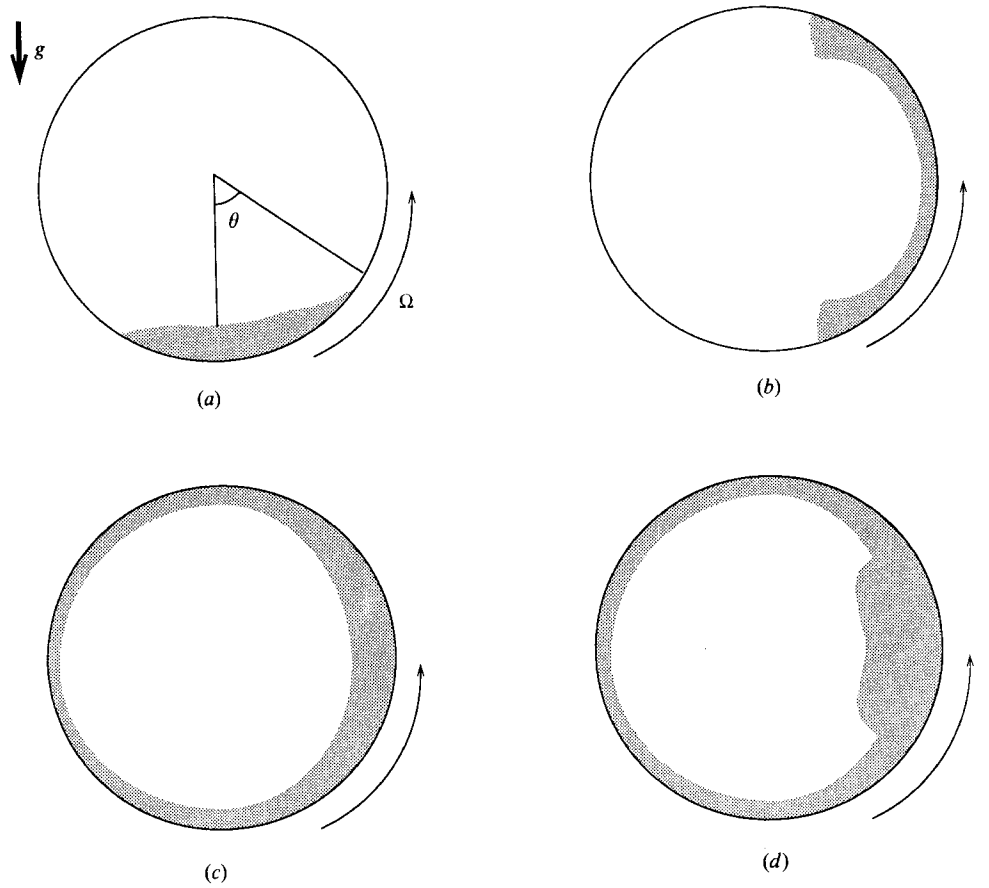

FIGURE 1. Sketch of four possible steady-state film configurations.

number limit for the case of a Newtonian fluid, but they derived an erroneous equation for the coating thickness and as a result they did not identify some of the many interesting film profiles and other features that will be described later. Other background information about flow inside rotating cylinders, not directly relevant to the present paper, can be found in Karweit & Corrsin (1975), Balmer (1970), Debler & Yih (1962), Phillips (1960), White (1956) and White & Higgins (1958). In addition, the present work has a great deal in common with the general subject of exterior coating flows for which there is a vast literature and the reader is referred to the review article by Ruschak (1985).

Here we consider the limit of a thin liquid coating using the well-known lubrication approximation. We do not restrict attention to Newtonian fluids or to rimming flows alone, but we consider power-law fluids and also investigate partial coatings. In fact, four distinct steady-state film configurations are identified, two of which only partially coat the cylinder surface and the other two, called continuous films or rimming flows, cover the entire cylinder surface. A rough sketch of typical examples for each of the four configurations is shown in figure 1; other variations will be discussed later.

Of the two partial films one corresponds to the appropriate solution valid for small rotation rates and not surprisingly the liquid or charge remains in a slightly

perturbed puddle at the bottom of the cylinder (e.g. figure 1*a*). This limit is not particularly interesting in terms of material processing and hence it shall not be explored in detail. The other partial film configuration consists of a film located on the ascending side of the rotating cylinder (e.g. figure 1*b*) and it is found to be a possible steady-state solution for a limited range of liquid volumes. For this case the portion of the cylinder surface covered by the film is a function of the liquid volume and the maximum possible volume corresponds to a film extending from the top ($\theta = \pi$) to the bottom ($\theta = 0$) of the cylinder along the rising side.

New results for rimming flows which have not been reported elsewhere are also presented. One interesting feature of rimming flows is the presence of two possible configurations. The first of these involves the somewhat expected situation of a coating that gradually changes in thickness around the cylinder (e.g. figure 1*c*). This film is deeper on the ascending side of the cylinder and shallower on the descending side. The second case in this category is a film that has one or two rapid transitions in depth on the rising side of the cylinder and can have recirculating eddies present (e.g. figure 1*d*).

2. Analysis

Since many of the most interesting features of the flow to be discussed are exhibited by Newtonian fluids and since the presentation is particularly simple in this case, we will begin by considering this case first. The extension to power-law fluids will be presented later. We consider a horizontal circular cylinder of inside radius R which rotates at a constant angular velocity Ω about its axis as shown in figure 1. The thickness of the fluid coating is taken to be $\hat{h}(\theta)$, where θ is the azimuthal coordinate, with the bottom of the cylinder being at $\theta = 0$ and θ increasing in a counterclockwise sense. It is convenient to express the radial coordinates as $\hat{r} = R - \hat{n}$, where $\hat{n}$ is a new radial coordinate measured from the inner wall of the cylinder (a caret denotes dimensional quantities). Making the assumption that the fluid coating is thin amounts to requiring the parameter $\delta = h_0/R$ to be much less than unity, where h_0 is the characteristic thickness of the film. Naturally, the thinness assumption is equivalent to assuming that the volume of the charge in the rotating mould is small. We introduce dimensionless velocities in the radial and azimuthal directions:

$$u_r = \hat{u}_r/\delta\Omega R, \quad u_\theta = \hat{u}_\theta/\Omega R,$$

and the scale the radial coordinate $\hat{r}$ by the cylinder radius R and the coordinate $\hat{n}$ by h_0, i.e.

$$r = \hat{r}/R = 1 - \hat{n}/R = 1 - \delta n, \quad n = \hat{n}/h_0.$$

The normal stresses, pressure and deviatoric stresses are made dimensionless by

$$\tau_{rr} = \hat{\tau}_{rr}/(\mu\Omega/\delta), \quad \tau_{\theta\theta} = \hat{\tau}_{\theta\theta}/(\mu\Omega/\delta), \quad p = \hat{p}/(\mu\Omega/\delta), \quad s_{ij} = \hat{s}_{ij}/(\mu\Omega/\delta),$$

where $\hat{\tau}_{ij} = \frac{1}{2}\hat{\tau}_{kk}\,\delta_{ij} + \hat{s}_{ij}$ and μ is the dynamic viscosity of the fluid. Consequently, assuming that the Froude number $(\Omega^2 R/g)^{\frac{1}{2}}$ is small and therefore neglecting inertial effects the governing equations become

$$-\delta\frac{\partial\tau_{rr}}{\partial n} + \frac{\delta^2}{1-\delta n}\frac{\partial s_{r\theta}}{\partial\theta} + \frac{2\delta^2}{1-\delta n}s_{rr} + \delta\Gamma\cos\theta = 0, \tag{1}$$

$$-\frac{\partial s_{r\theta}}{\partial n} + \frac{\delta}{1-\delta n}\frac{\partial\tau_{\theta\theta}}{\partial\theta} + \frac{2\delta}{1-\delta n}s_{r\theta} - \Gamma\sin\theta = 0, \tag{2}$$

and conservation of mass for an incompressible fluid is

$$-\frac{\partial u_r}{\partial n}+\frac{\delta}{1-\delta n}u_r+\frac{1}{1-\delta n}\frac{\partial u_\theta}{\partial \theta}=0. \tag{3}$$

Note that we have used $\tau_{rr}-\tau_{\theta\theta}=2s_{rr}$ in (1) and we define

$$\Gamma=\delta^2\rho g R/\mu\Omega, \tag{4}$$

where Γ^{-1} is a product of the square of the Froude number and an Ekman number based on the film thickness, i.e. $\mu/\rho\Omega h_0^2$.

For the Newtonian fluid the material behaviour is given in dimensional quantities by

$$\hat{s}_{ij}=2\mu\hat{e}_{ij},$$

where $\hat{e}_{ij}$ is the strain rate and $\hat{s}_{ij}$ is the deviatoric stress, and we find the dimensionless constitutive equations to be

$$-\delta\frac{\partial u_r}{\partial n}=\tfrac{1}{2}s_{rr}, \tag{5}$$

$$\frac{\delta}{1-\delta n}\frac{\partial u_\theta}{\partial \theta}+\frac{\delta^2}{1-\delta n}u_r=\tfrac{1}{2}s_{\theta\theta}, \tag{6}$$

$$-\frac{\partial u_\theta}{\partial n}-\frac{\delta}{1-\delta n}u_\theta+\frac{\delta^2}{1-\delta n}\frac{\partial u_r}{\partial \theta}=s_{r\theta}. \tag{7}$$

Note that the somewhat unconventional formulation involving the stresses is not typically used for Newtonian fluids, but it will make the extension to power-law fluids straightforward.

We consider $\Gamma=O(1)$ and retain the leading terms for small δ in (1), (2) and (3):

$$\frac{\partial \tau_{rr}}{\partial n}\approx\Gamma\cos\theta, \tag{8}$$

$$\frac{\partial s_{r\theta}}{\partial n}-2\delta s_{r\theta}\approx\delta\frac{\partial \tau_{\theta\theta}}{\partial \theta}-\Gamma\sin\theta, \tag{9}$$

$$-\frac{\partial u_r}{\partial n}+\frac{\partial u_\theta}{\partial \theta}\approx 0 \tag{10}$$

(note that $O(\delta)$-terms in (9) have been retained for later use when we examine transition solutions in regions where the film thickness changes rapidly). At leading order the constitutive equations become

$$s_{rr}\approx 0, \tag{11}$$

$$s_{\theta\theta}\approx 0, \tag{12}$$

$$\frac{\partial u_\theta}{\partial n}\approx -s_{r\theta}, \tag{13}$$

and we see that at leading order the longitudinal deviatoric stresses vanish. This is the standard result of lubrication theory, namely, that the flow is dominated by shear stresses and pressure. From (8) we find

$$\tau_{rr}=\Gamma\cos\theta[n-h(\theta)],$$

where we have applied the normal stress boundary condition $\tau_{rr} \approx 0$ on the free surface $n = h(\theta)$ (note that this is the leading-order boundary condition on the normal stress for small δ). We have neglected surface tension and any dynamical effect of the gas in the cylinder above the free surface. Furthermore, using (11) we have $\tau_{rr} = \tau_{\theta\theta} + 2s_{rr} \approx \tau_{\theta\theta}$, and (9) becomes

$$\frac{\partial s_{r\theta}}{\partial n} - 2\delta s_{r\theta} \approx \delta \frac{\partial \tau_{rr}}{\partial \theta} - \Gamma \sin\theta = -\Gamma\left\{[1+\delta(n-h)]\sin\theta + \delta\frac{\mathrm{d}h}{\mathrm{d}\theta}\cos\theta\right\}.$$

Letting $s_{r\theta} = s_{r\theta}^{(0)} + \delta s_{r\theta}^{(1)} + \ldots$ and substituting in the above we can readily evaluate the first- and second-order terms in the shear stress. On the free surface $n = h(\theta)$ the shear stress vanishes and therefore we apply the condition $s_{r\theta} \approx 0$ to ultimately find

$$s_{r\theta} = -\Gamma(n-h)\left\{[1+\tfrac{3}{2}\delta(n-h)]\sin\theta + \delta\frac{\mathrm{d}h}{\mathrm{d}\theta}\cos\theta\right\}. \tag{14}$$

Substituting the expression for the shear stress into (7) gives

$$\frac{\partial u_\theta}{\partial n} + \delta u_\theta = \Gamma(n-h(\theta))\left\{[1-\tfrac{3}{2}\delta(h-n)]\sin\theta + \delta\frac{\mathrm{d}h}{\mathrm{d}\theta}\cos\theta\right\}, \tag{15}$$

which may be integrated to find the azimuthal velocity u_θ. After obtaining u_θ from (15) using the condition $u_\theta = 1$ on $n = 0$, the mass conservation equation (10) then determines the radial component of velocity using the condition that $u_r = 0$ on $n = 0$. The details of this calculation are not important for the present discussion so they will be omitted for the sake of brevity.

Lastly, integrating the equation of mass conservation across the film from $n = 0$ to h and applying the condition $u_r(n = 0) = 0$ and that the normal component of velocity vanishes on the free surface, i.e. $u_r + u_\theta \mathrm{d}h/\mathrm{d}\theta \approx 0$ on $n = h(\theta)$, gives the equation

$$\frac{\mathrm{d}}{\mathrm{d}\theta}\int_0^{h(\theta)} u_\theta \,\mathrm{d}n = 0. \tag{16}$$

This states that the volume flow rate per unit length, q, is conserved for a steady-state film, i.e.

$$q = \int_0^{h(\theta)} u_\theta \,\mathrm{d}n = \text{const}. \tag{17}$$

This equation determines the film profile $h(\theta)$. For a Newtonian fluid the expressions for u_θ and q are

$$u_\theta = 1 - \delta n - \Gamma\left\{\left(\sin\theta + \delta\frac{\mathrm{d}h}{\mathrm{d}\theta}\cos\theta\right)n(h-\tfrac{1}{2}n) - \delta n(\tfrac{3}{2}h^2 - nh + \tfrac{1}{3}n^2)\sin\theta\right\}, \tag{18}$$

$$q = h - \tfrac{1}{2}\delta h^2 - \tfrac{1}{3}\Gamma h^3\left[\sin\theta + \delta\frac{\mathrm{d}h}{\mathrm{d}\theta}\cos\theta - \tfrac{3}{2}\delta h\sin\theta\right]. \tag{19}$$

2.1. *Continuous films – Newtonian fluids*

For a continuous film covering the entire surface, we determine the profile of the film $h(\theta)$ from (17) and (19). Neglecting terms of $O(\delta)$ we have

$$q = h - \tfrac{1}{3}\Gamma h^3 \sin\theta = \text{const} = h(0). \tag{20}$$

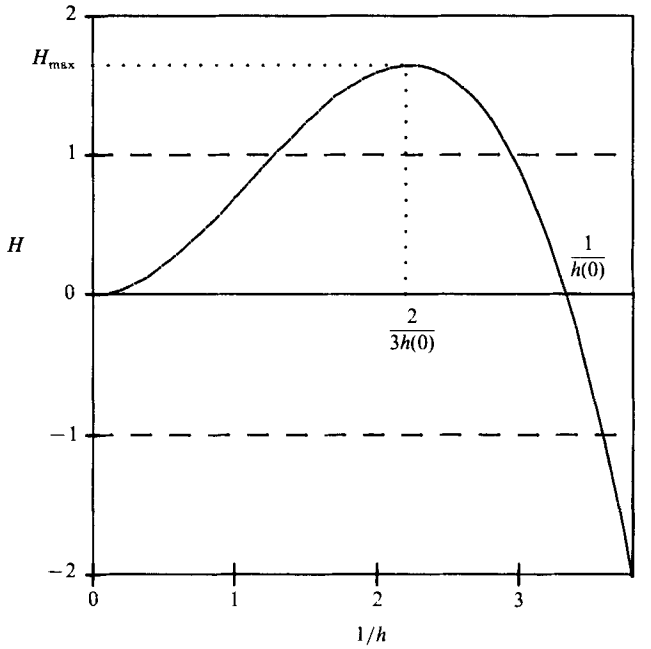

FIGURE 2. Sketch of the function $H = (1/h^2)[1-h(0)/h]$ versus $1/h$ (see equation (22)). Note that for a Newtonian fluid $H_{max} = 4/[27h^2(0)]$ and recall that $h(\theta)$ is given implicitly by $\sin\theta = H(h^{-1})$. The general shape of the curve $H(h^{-1})$ is similar for power-law fluids.

Now recall that $\Gamma = \delta^2\rho gR/\mu\Omega$, where $\delta = h_0/R$ and that we have not yet specified the characteristic film thickness h_0 precisely. Consequently it is convenient here to choose h_0 such that $\frac{1}{3}\Gamma = 1$, i.e. $\delta^2 = 3\mu\Omega/\rho gR$ and therefore $h_0 = (3\mu\Omega/\rho gR)^{\frac{1}{2}}R$. We therefore wish to solve for $h(\theta)$ from

$$h - h^3\sin\theta = h(0). \tag{21}$$

It is useful to write this as

$$\sin\theta = \frac{1}{h^2}\left[1 - \frac{h(0)}{h}\right] = H(h^{-1}), \tag{22}$$

and examine the right-hand side versus $1/h$, which is sketched in figure 2. For $0 \leqslant \theta \leqslant 2\pi$ the left-hand side of (22) is between -1 and $+1$. Therefore, in order to have a positive real solution for $h(\theta)$ for all θ between 0 and 2π, i.e. a continuous film, $H(h^{-1})$, must extend from $+1$ to -1 (this situation is shown in figure 2). However, $H(h^{-1})$ has a maximum value $H_{max} = 4/[27h^2(0)]$ at $h = \frac{3}{2}h(0)$ and therefore we see that a continuous film is only possible if $H_{max} \geqslant 1$, or equivalently if $h(0) \leqslant 2/3^{\frac{3}{2}}$. If this is not the case then we do not have a real, positive solution for $h(\theta)$ in a region bordering around $\theta = \frac{1}{2}\pi$.

Limiting our attention for the moment to continuous films and therefore assuming that we have $h(0) \leqslant 2/3^{\frac{3}{2}}$ (i.e. $H_{max} \geqslant 1$), we can see from figure 2 that (22) has two positive, real roots $h(\theta)$ for $0 \leqslant \theta \leqslant \pi (0 \leqslant H \leqslant 1)$ and only one positive real root for $\pi \leqslant \theta \leqslant 2\pi (-1 \leqslant H \leqslant 0)$. Consequently, (21) predicts two rather distinct steady-state continuous-film configurations and the two cases have markedly different film profiles on the rising side of the cylinder between $\theta = 0$ and π. The two thicknesses predicted on the rising side of the cylinder are analogous to the two solutions found

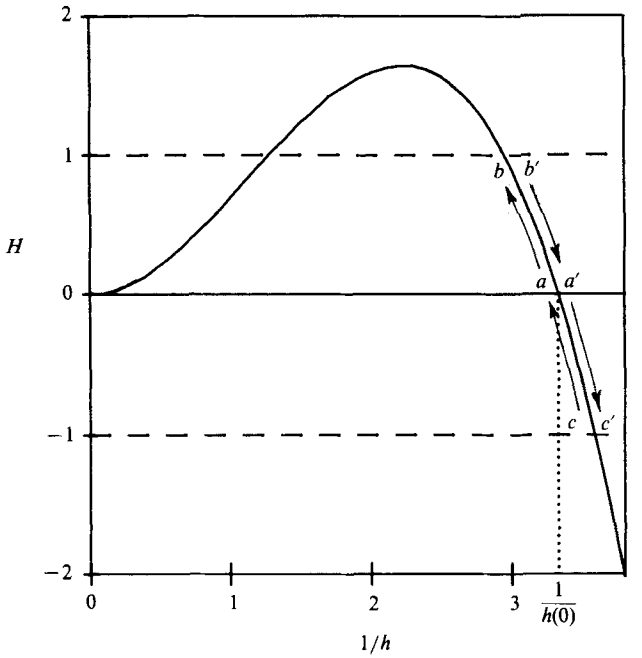

FIGURE 3. Locus of points $h(\theta)$ which represent a continuous film or rimming flow as shown in the sketch in figure 1(*c*) (see text for discussion).

in dip coating or free-withdrawal coating in which a solid surface is withdrawn from a reservoir (Ruschak 1985; Van Rossum 1958; Tuck 1983). In dip coating on a vertical surface it is generally believed that the coating thickness corresponds to the film with the greatest volume flux, in which case the two solutions coincide (in the present notation this corresponds to $\sin\theta = 1$, $H_{\max} = 1$, $q = h(0) = 2/3^{\frac{3}{2}}$ and $h = 1/\sqrt{3}$). Here, however, we show how the two distinct depths can be used to construct interesting steady-state flows involving rapid changes in depth.

Of the two continuous film types, the first and somewhat expected continuous film profile is a gently varying profile (e.g. figure 1*c*) and can be obtained from the solution path for increasing θ shown by the arrows in figure 3. In figure 3 we begin at point a where the curve $H(h^{-1})$ crosses the $1/h$ axis where $\theta = 0$, $(H = 0)$ and $h = h(0)$. As we proceed from point a to b, θ increases and the film thickens ($1/h$ decreases) and a maximum thickness $h(\theta)$ is reached at point b where $\theta = \frac{1}{2}\pi$ $(H = 1)$. Then from point b' to c' the film thins as θ increases and at c' we have $\theta = \frac{3}{2}\pi$ $(H = -1)$ and $h(\theta)$ is a minimum. From point c to a or equivalently from $\theta = \frac{3}{2}\pi$ to 2π the film thickens and returns to its original value $h(0)$. A few specific examples of the resulting film profiles for various values of $h(0)$ are shown in figure 4. As $h(0)$ increases, the variation in the film thickness increases owing to the increasing influence of the gravity force. Note that the thickest film shown corresponds to the solution when $h(0)$ equals its maximum value $2/3^{\frac{3}{2}} = 0.385$.

A second and somewhat unexpected continuous-film configuration predicted by (21) would result from a solution path such as that shown by the arrows in figure 5; namely, as θ increases from 0 at point a, $h(\theta)$ would be increasing and then at some $\theta = \theta^* \leqslant \frac{1}{2}\pi$ (point b) the film thickness would jump rather suddenly in depth from h_1 (at point b) to h_2 (at point c). The film would then thin as θ increased to $\frac{1}{2}\pi$ (point

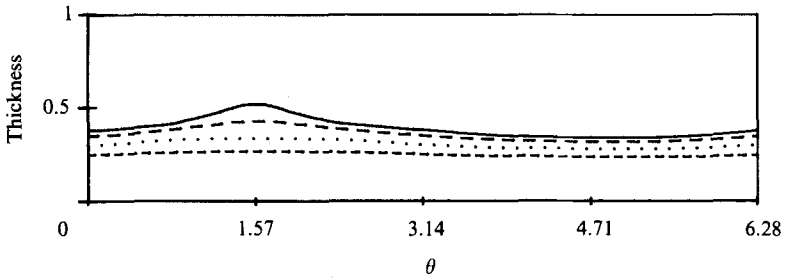

FIGURE 4. Continuous film profiles for a Newtonian fluid; $h(\theta)$ versus θ. ——, $h(0) = 0.38$; ——, 0.35; · · ·, 0.30; – – –, 0.25.

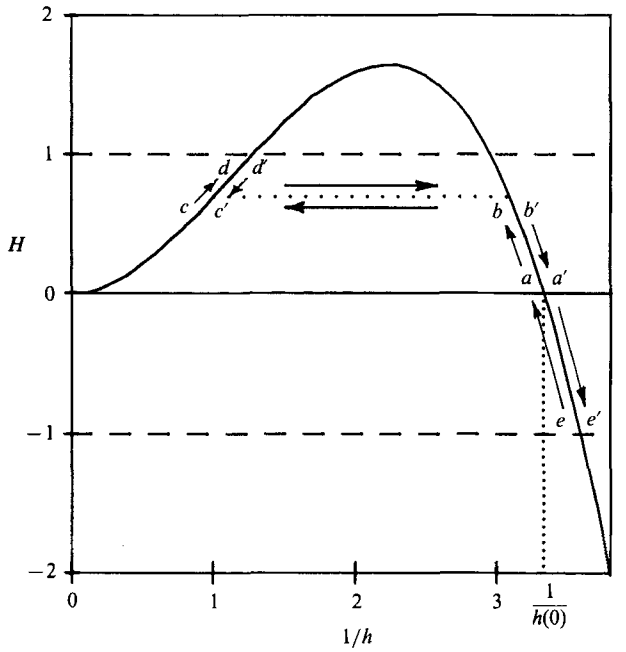

FIGURE 5. Locus of points $h(\theta)$ which describe a continuous film having two rapid transitions as shown in the sketch in figure 1 (*d*).

d) and then would increase in thickness for $\frac{1}{2}\pi < \theta < \pi - \theta^*$. At point c' where $\theta = \pi - \theta^*$ the film would suddenly thin from h_2 to h_1 (from c' to b') and it would continue to thin more gradually as θ increased to $\frac{3}{2}\pi$ at point e'. Lastly, from $\theta = \frac{3}{2}\pi$ (point e) to $\theta = 2\pi$ (point a) the film would thicken and return to its starting value $h(0)$. A sketch of this general situation is shown in figure 1 (*d*). The sudden transitions predicted in this case are, of course, regions of non-uniformity of the present solution. The transition is not a sudden jump in thickness but a rapid smooth transition between the two depths. This transition can be evaluated by returning to (19) and reinstating the term $\delta\, \mathrm{d}h/\mathrm{d}\theta$ which is not negligible in these transition regions since $\mathrm{d}h/\mathrm{d}\theta$ becomes large. As will be seen below, this thick region near $\theta = \frac{1}{2}\pi$ is often a recirculating zone of trapped fluid and fluid moving with the rotating cylinder is passing underneath this thick zone. The solution described above is only one of a number of possible cases, many of which will be described later. Lastly, the films

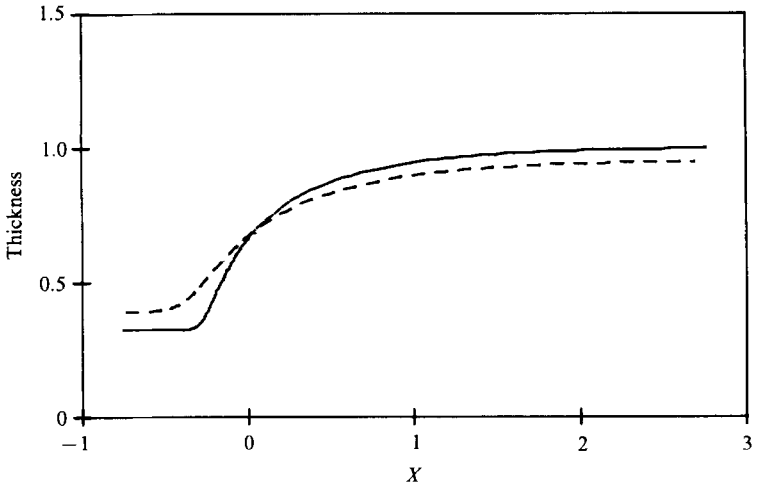

FIGURE 6. Structure of the rapid transition, i.e. h versus X, for $\theta^* \approx \frac{1}{4}\pi$: ---, $h(0) = 0.35$; ——, 0.30.

involving a rapid change in depth found here are somewhat reminiscent of the films involving a change in depth found in jet-stripping by Tuck (1983).

The precise structure of the transition regions is easily illustrated for the case of a Newtonian fluid whereby we must return to (19) and consider

$$q = h\left[1 - h^2\left(\sin\theta + \delta\cos\theta\frac{\mathrm{d}h}{\mathrm{d}\theta}\right)\right] = h(0). \tag{23}$$

If a transition point is present at $\theta = \theta^*$, then after introducing the inner variable $X = (\theta - \theta^*)/\delta$ the equation for the transition or inner solution becomes

$$\cos\theta^*\frac{\mathrm{d}h}{\mathrm{d}X} = \frac{1}{h^2}\left(1 - \frac{h(0)}{h}\right) - \sin\theta^* = H(h^{-1}) - \sin\theta^*. \tag{24}$$

Since $H(h^{-1}) - \sin\theta^* \geqslant 0$ for $h_1 < h < h_2$ (see figure 5) we see that for $0 \leqslant \theta^* < \frac{1}{2}\pi$ (i.e. $\cos\theta^*$ positive), $\mathrm{d}h/\mathrm{d}X$ is positive and therefore (24) describes a film increasing in thickness. For $\frac{1}{2}\pi < \theta^* \leqslant \pi$, $\mathrm{d}h/\mathrm{d}X$ is negative and (24) describes a thinning transition which is simply the mirror image of the transition for $0 \leqslant \theta^* < \frac{1}{2}\pi$. Furthermore, the solution to (24) will match to the outer solution. For $0 \leqslant \theta^* < \frac{1}{2}\pi$, as $X \to -\infty$ we have $\mathrm{d}h/\mathrm{d}X \to 0$ and $h \to h_1$ and as $X \to +\infty$, $\mathrm{d}h/\mathrm{d}X \to 0$ and $h \to h_2$. Similarly, for $\frac{1}{2}\pi < \theta^* \leqslant \pi$, $\mathrm{d}h/\mathrm{d}X \to 0$ and $h \to h_2 > h_1$ as $X \to -\infty$, and $\mathrm{d}h/\mathrm{d}X \to 0$ and $h \to h_1$ as $X \to +\infty$. Equation (24) is easily integrated numerically and two typical examples of the transition solution are shown in figure 6. Note that as $h(0)$ decreases the initial increase in depth is very rapid compared with the more gentle approach to h_2 as $X \to \infty$. This region of high curvature is surely a region where surface-tension effects would become important, tending to smooth out the transition somewhat. However, we have not considered surface-tension effects in the present work. In figure 7 the overall film profile for $0 \leqslant \theta \leqslant 2\pi$ is plotted for a few typical cases, i.e. the uniformly valid solution $h(\theta)$ obtained from (24) and (21) is plotted for $\theta^* \approx \frac{1}{4}\pi$, and $h(0) = 0.30$, 0.28 and 0.25. The dotted lines in these figures denote a recirculating zone which is discussed below.

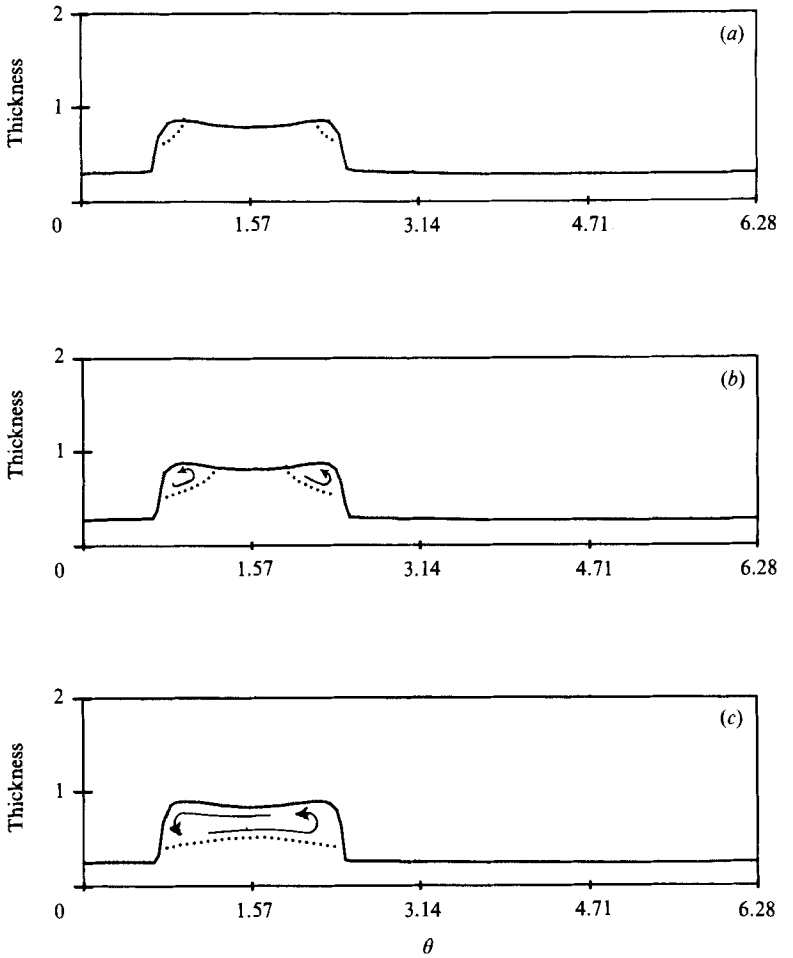

FIGURE 7. Typical Newtonian fluid film profiles, $h(\theta)$ versus θ, for films having two transitions located symmetrically about $\theta = \frac{1}{2}\pi$ ($\theta^* = \frac{1}{4}\pi$): (*a*) $h(0) = 0.30$; (*b*) 0.28; (*c*) 0.25. The dotted line denotes the streamline bounding the recirculating zones in each case.

Another interesting feature of the continuous-film solution is obtained by examining (18) for u_θ. Clearly, for $0 \leqslant \theta \leqslant \pi$ the azimuthal velocity u_θ has the potential to change sign, that is, a recirculating zone is possible on the rising side of the rotating cylinder. The presence of a recirculating zone is easily identified by determining the stagnation points on the surface $n = h(\theta)$, i.e.

$$u_\theta(n = h, \theta) = 0 = 1 - \tfrac{3}{2}\sin\theta h^2, \tag{25}$$

recalling that we chose $\frac{1}{3}\Gamma = 1$ and noting that $O(\delta)$-terms have been neglected. Equation (25) can only vanish for $0 \leqslant \theta \leqslant \pi$ and the stagnation points $\theta = \theta_s$ are given by

$$h^2(\theta_s)\sin\theta_s = \tfrac{2}{3}. \tag{26}$$

Substituting this in (21) for $h(\theta)$ we find

$$h(\theta_s) = 3h(0). \tag{27}$$

Consequently, (26) gives the stagnation-point locations θ_s as

$$\sin\theta_s = \frac{2}{27h^2(0)}.$$

Therefore, two recirculating zones are present and positioned symmetrically about $\theta = \frac{1}{2}\pi$ when $2/27h^2(0) \leqslant 1$ or equivalently when

$$h(0) \geqslant \frac{\sqrt{2}}{3\sqrt{3}} \tag{28}$$

Note that the stagnation points move towards $\theta = \frac{1}{2}\pi$ as $h(0)$ approaches the minimum value given in (28).

Now, recall that the function $H(h^{-1})$ has a maximum at $h = \frac{3}{2}h(0)$ (see figure 2) and therefore the continuous-film solutions which do not have jumps correspond to values of $h(\theta)$ that satisfy $h(\theta) \leqslant \frac{3}{2}h(0)$ for all θ. Consequently, since the stagnation points are located at $h(\theta_s) = 3h(0)$ which is greater than $\frac{3}{2}h(0)$, clearly the presence of recirculating zones is restricted to films having rapid transitions or jumps. However, recirculating zones are not always present, but will occur only when the greater of the two depths at the transition point $\theta = \theta^*$, i.e. h_2, is greater than $h(\theta_s) = 3h(0)$ given by (27); otherwise there is a jump but no recirculation zones. Furthermore, when jumps are present and $h(0)$ is less than the minimum value given in (28) we find that a single large recirculation zone is present which extends between the two jumps. The separating streamlines shown in figure 7 are easily evaluated by computing the volume flow rate between the cylinder wall $n = 0$ and a position $n = n_s(\theta)$, and requiring that this flow rate equal the flow rate through the film between π and 2π, i.e. $q(0) = h(0)$,

$$q(n_s) = \int_0^{n_s} u_\theta \, dn = h(0),$$

giving

$$h(0) = n_s - \tfrac{3}{2}\sin\theta h^3\left[\frac{2}{3} - \left(1 - \frac{n_s}{h}\right) + \frac{1}{3}\left(1 - \frac{n_s}{h}\right)^3\right].$$

This equation is easily solved for n_s using Newton's method. From figure 7 we see that the thick regions are often trapped recirculating zones which are underrun by fluid being dragged along by the rotating cylinder.

Lastly, note that the actual number of possible film configurations involving rapid transitions are limitless. In the preceding discussion we examined two transitions located symmetrically about $\theta = \frac{1}{2}\pi$; however, any conceivable non-symmetric configuration is also possible so that the film profile on the rising side of the cylinder need not be symmetric. In figure 7 we have only attempted to illustrate one of many possible film configurations. Other possible configurations (e.g. figure 11) will be described in §3.

2.2. *Partial films – Newtonian fluids*

For a film of limited extent (e.g. figure 1*b*) clearly the volume flux must vanish and so the equation for $h(\theta)$ becomes

$$q = h - \tfrac{1}{3}\Gamma h^3 \sin\theta = 0.$$

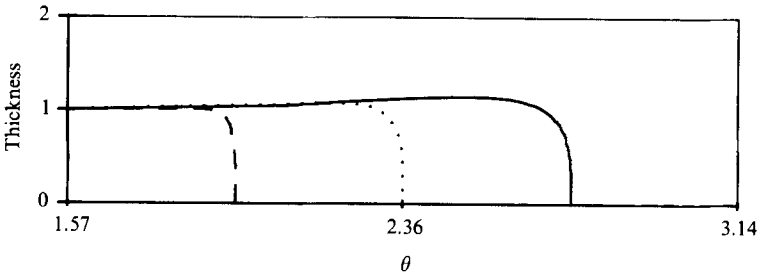

FIGURE 8. Typical partial film profiles for a Newtonian fluid: ——, $\theta_0 = \frac{7}{8}\pi$; · · ·, $\frac{3}{4}\pi$; – – –, $\frac{5}{8}\pi$.

Once again it is sensible to choose h_0 such that $\frac{1}{3}\Gamma = 1$ and we have a positive, real solution for h only for $0 \leqslant \theta \leqslant \pi$ and hence

$$h = \left[\frac{1}{\sin\theta}\right]^{\frac{1}{2}}. \tag{29}$$

However, this solution does not satisfy the required condition on a partial film, namely, that $h = 0$ at specified locations. Therefore, we need to incorporate transition solutions which describe the edges of the film. This, once again, requires reinstating the term $\delta\,\mathrm{d}h/\mathrm{d}\theta$ in (19) and we must consider

$$q = h - \tfrac{1}{3}\Gamma h^3\left(\sin\theta + \delta\cos\theta\frac{\mathrm{d}h}{\mathrm{d}\theta}\right) = 0, \tag{30}$$

giving (note $\frac{1}{3}\Gamma = 1$)

$$\delta\cos\theta h^2\frac{\mathrm{d}h}{\mathrm{d}\theta} + h^2\sin\theta = 1. \tag{31}$$

Suppose the contact line where the film vanishes is located at $\theta = \theta_0$, then let $X = (\theta - \theta_0)/\delta$ and consider

$$\cos\theta_0 h^2\frac{\mathrm{d}h}{\mathrm{d}X} + h^2\sin\theta_0 = 1, \tag{32}$$

giving

$$X = \cos\theta_0\int_0^h \frac{h^2\,\mathrm{d}h}{1 - h^2\sin\theta_0},$$

$$X = \frac{\cos\theta_0}{\sin\theta_0}\left\{-h + \int_0^h \frac{\mathrm{d}h}{1 - h^2\sin\theta_0}\right\}. \tag{33}$$

Naturally, as $h \to (1/\sin\theta_0)^{\frac{1}{2}}$, i.e. the inner limit of the outer solution equation (29), we find from (33) that $X \to +\infty$ as required. For a Newtonian fluid we can evaluate (33) explicitly as

$$\theta = \theta_0 + \cot\theta_0\left\{-h + \frac{1}{2\sin^{\frac{1}{2}}\theta_0}\ln\left[\frac{1 + h\sin^{\frac{1}{2}}\theta_0}{1 - h\sin^{\frac{1}{2}}\theta_0}\right]\right\}. \tag{34}$$

A few typical film profiles obtained from (34) and (29) are shown in figure 8 for $\frac{1}{2}\pi \leqslant \theta \leqslant \pi$ (note that the film must straddle $\theta = \frac{1}{2}\pi$ and only part of the film is shown). As we approach the contact line we see from (32) that, as $X \to 0$,

$$h \propto X^{\frac{1}{3}},$$

and

$$\frac{\mathrm{d}h}{\mathrm{d}X} \propto X^{-\frac{2}{3}} \to \infty,$$

and the end of the film is very blunt. Note that if we wanted to satisfy a prescribed contact-angle condition, it would be necessary to return to the original formulation and include surface-tension effects. In reality a further non-uniformity exists in the solution and very close to the contact line surface-tension effects play an important role. For a survey of the many papers that have dealt with this issue, particularly for Newtonian fluids, see Davis (1983).

A second partial-film configuration exists which corresponds to the appropriate solution for small rotation rates Ω. In this case it is not desirable to choose the characteristic thickness h_0 such that $\frac{1}{3}\Gamma = 1$ (where $\Gamma = \delta^2 \rho g R/\mu\Omega$). Instead we wish to examine the solution for Ω small and therefore $\Gamma \gg 1$. Consequently, retaining the leading-order terms for large Γ in (30) we have

$$q = h^3\left(\sin\theta + \delta\cos\theta\frac{\mathrm{d}h}{\mathrm{d}\theta}\right) + O\left(\frac{1}{\Gamma}\right) = 0. \tag{35}$$

This leading-order equation describes a static film, and higher-order corrections begin to account for the weak rotation of the cylinder. Basically the situation consists of a perturbed puddle at the bottom of the cylinder. The static-film solution obtained from (35) is given by

$$h = h(0) + \delta^{-1}\ln(\cos\theta), \tag{36}$$

where it is appropriate to take the characteristic film thickness $h_0 = \hat{h}(0)$ so that $h(0) = \hat{h}(0)/h_0 = 1$ and, in order to have a thin film, clearly the extent of the film must be small, i.e. $\theta = O(\delta^{\frac{1}{2}})$. For θ small, we then have

$$h \simeq 1 - \tfrac{1}{2}\delta^{-1}\theta^2 + \ldots \tag{37}$$

and the contact line is located at $\theta_0 \approx (2\delta)^{\frac{1}{2}} + \ldots$. Higher-order corrections in Γ^{-1} accounting for the motion are easily obtained, but they are not very interesting physically so we shall not discuss them further. Note that for small Ω it is also possible to construct the perturbation solution when the film is not thin; the merit in doing this, however, is not clear.

Along the same lines, it is also not appropriate to take $\frac{1}{3}\Gamma = 1$ when Ω is large. In this case we can consider $\Gamma \ll 1$ and develop a perturbation solution to (20) which describes a rimming flow,

$$h \approx h(0) + \tfrac{1}{3}\Gamma h^3(0)\sin\theta + O(\Gamma^2), \tag{38}$$

and hence the film thickness $h(\theta)$ in this case is nearly constant. This is a near rigid-body rotation and falls among the class of rimming flows considered by Rushak & Scriven (1976).

2.3. *Extension to power-law fluids*

The power-law description of the material behaviour that replaces the Newtonian behaviour is given in dimensional quantities by

$$\hat{e}_{ij} = B\hat{\tau}^{m-1}\hat{s}_{ij},$$

where $\hat{\tau}^2 = \frac{1}{2}\hat{s}_{ij}\hat{s}_{ij}$, and B and m are material parameters ($m \geqslant 1$). Naturally $m = 1$ corresponds to the Newtonian-fluid case where $B^{-1} = 2\mu$. Making the deviatoric

stresses dimensionless as before, we find the dimensionless constitutive equations to be

$$-\delta\frac{\partial u_r}{\partial n} = \tfrac{1}{2}\tau^{m-1}s_{rr}, \tag{39}$$

$$\frac{\delta}{1-\delta n}\frac{\partial u_\theta}{\partial\theta}+\frac{\delta^2}{1-\delta n}u_r = \tfrac{1}{2}\tau^{m-1}s_{\theta\theta}, \tag{40}$$

$$-\frac{\partial u_\theta}{\partial n}-\frac{\delta}{1-\delta n}u_\theta+\frac{\delta^2}{1-\delta n}\frac{\partial u_r}{\partial\theta} = \tau^{m-1}s_{r\theta}, \tag{41}$$

where the viscosity μ used in the non-dimensionalization is an effective viscosity given by

$$\mu = \frac{1}{2}\left(\frac{\delta}{\Omega}\right)^{1-1/m}\frac{1}{B^{1/m}}.$$

Owing to incompressibility note that $s_{rr} = -s_{\theta\theta}$ and therefore $\tau^2 = s_{\theta\theta}^2 + s_{r\theta}^2$.

At this point the analysis proceeds exactly as before with the one exception that now

$$\frac{\partial u_\theta}{\partial n}+\delta u_\theta \approx -\tau^{m-1}s_{r\theta}, \tag{42}$$

and since the longitudinal deviatoric stresses vanish at leading order we have $\tau^2 \approx s_{r\theta}^2$. The shear stress is unchanged and given again by (14). Substituting the expression for shear stress into (42) gives an equation for the azimuthal velocity

$$\frac{\partial u_\theta}{\partial n}+\delta u_\theta = \Gamma|s_{r\theta}|^{m-1}(n-h(\theta))\left\{[1-\tfrac{3}{2}\delta(h-n)]\sin\theta+\delta\frac{\mathrm{d}h}{\mathrm{d}\theta}\cos\theta\right\}. \tag{43}$$

As before the radial component of velocity is determined from mass conservation.

For arbitrary values of m the integration of (43) for u_θ is somewhat cumbersome, however, for small δ, (43) can be approximated by

$$\frac{\partial u_\theta}{\partial n} = \Gamma|s_{r\theta}|^{m-1}(n-h(\theta))\sin\theta = \Gamma^m \operatorname{sgn}(\sin\theta)|\sin^m\theta|(h-n)^m, \tag{44}$$

where $\operatorname{sgn}(\sin\theta)$ is $+1$ or -1 depending on the sign of $\sin\theta$.

Consequently, we find that

$$u_\theta = 1-\frac{\Gamma^m}{m+1}\operatorname{sgn}(\sin\theta)|\sin^m\theta|[h^{m+1}-(h-n)^{m+1}], \tag{45}$$

and

$$q = h-\frac{\Gamma^m}{m+2}h^{m+2}\operatorname{sgn}(\sin\theta)|\sin^m\theta|. \tag{46}$$

2.4. *Continuous films – power-law fluids*

For a continuous film covering the entire surface, we now have

$$q = h-\frac{\Gamma^m}{m+2}h^{m+2}\operatorname{sgn}(\sin\theta)|\sin^m\theta| = \text{const} = h(0). \tag{47}$$

Consequently, it is convenient here to choose h_0 such that $\Gamma^m/m+2 = 1$, i.e.

$$\delta^{1+1/m} = \tfrac{1}{2}[(m+2)\Omega/B]^{1/m}/\rho gR$$

and therefore
$$h_0 = [(m+2)\,\Omega/B]^{1/(m+1)}\,[1/2\rho g R]^{m/(m+1)}\,R,$$

and we determine $h(\theta)$ from

$$h - h^{m+2}\,\mathrm{sgn}\,(\sin\theta)\,|\sin^m\theta| = h(0),$$

or
$$\mathrm{sgn}\,(\sin\theta)\,|\sin^m\theta| = \frac{1}{h^{m+1}}\left[1-\frac{h(0)}{h}\right] = H(h^{-1}). \tag{48}$$

From this point on the discussion follows closely that for a Newtonian fluid and the reader is referred to §2.1 for a complete discussion. Since the general shape for $H(h^{-1})$ is essentially unchanged from that shown in the sketch in figure 2 the preceding discussion applies here and we shall only note the main differences between a power-law fluid and a Newtonian fluid. In the present case $H(h^{-1})$ has a maximum value,

$$H_{\max} = \frac{1}{m+2}\left[\frac{m+1}{(m+2)\,h(0)}\right]^{m+1} \quad \text{at } h = \frac{m+2}{m+1}h(0), \tag{49}$$

and therefore a continuous film is only possible if $H_{\max} \geqslant 1$, or equivalently if

$$h(0) \leqslant \frac{m+1}{(m+2)^{(m+2)/(m+1)}}. \tag{50}$$

Once again, (48) predicts two very different steady-state continuous-film configurations: one that gradually varies around the perimeter of the cylinder (see figure 3 and the discussion in §2.1) and one that rapidly changes in depth (see figure 5). Results for the film profiles of gradually varied continuous films are compared in figure 9 for $m = 1$ (Newtonian), 3 and 10. In each case the thickest film shown for each m corresponds to the maximum value of $h(0)$ noted in (50). Note that as m increases, variations in the film thickness decrease because velocity variations across the film are decreasing. In fact, as $m \to \infty$ the material behaves as a perfectly plastic material which would yield at the cylinder wall and flow as a slug with $u_\theta \approx 1$. In the case when jumps are present, the character of the film is similar to what was found for the Newtonian case and local transition solutions can also be constructed in the neighbourhood of the jumps.

Recirculating zones are also inherent in the solution in this case and, as we found before, they are present only when the film has rapid transition regions. The presence of two recirculating zones is identified by locating the stagnation points on the film surface where $u_\theta(h,\theta) = 0$. These locations are found for a power-law fluid to be given by

$$h(\theta_s) = (m+2)\,h(0),$$

and
$$\sin\theta_s = \left[\frac{m+1}{(m+2)^{m+2}h(0)^{m+1}}\right]^{1/m}. \tag{51}$$

Consequently, two recirculating zones are present when

$$h(0) \geqslant \frac{(m+1)^{1/(m+1)}}{(m+2)^{(m+2)/(m+1)}}. \tag{52}$$

As before, the recirculating zones are present only when the larger of the two depths at the transition point (h_2) is greater than the stagnation-point depth $h(\theta_s)$; otherwise a jump could be present but no recirculating zones would be found. When $h(0)$ is less

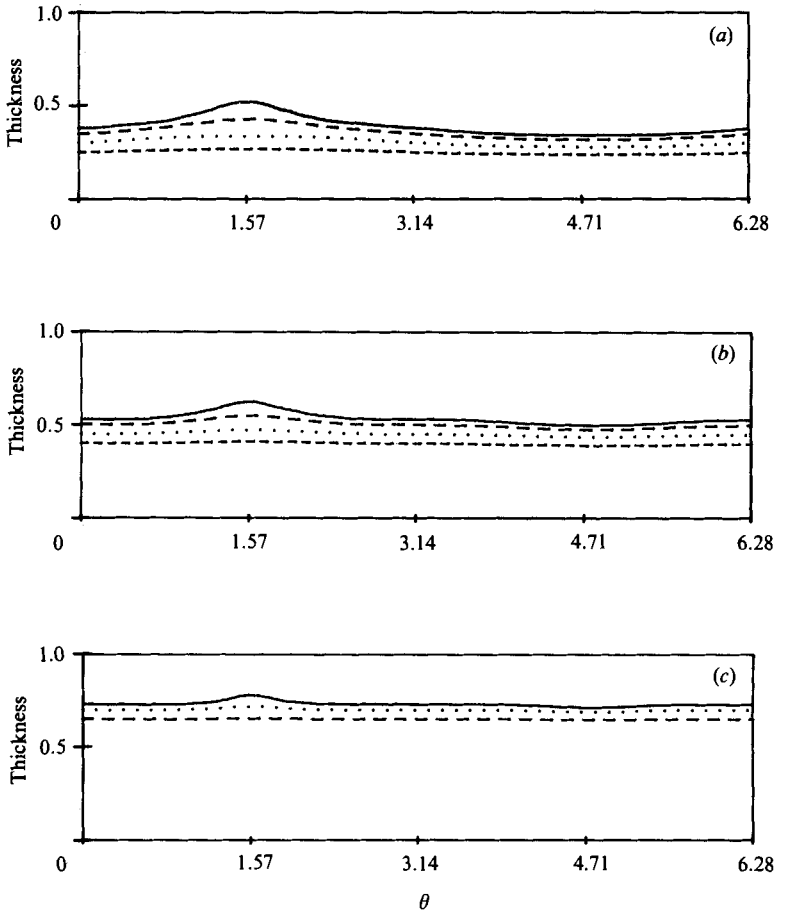

FIGURE 9. Continuous film profiles: $h(\theta)$ versus θ. (a) $m = 1$ (Newtonian fluid): ——, $h(0) = 0.38$; — —, 0.35; · · ·, 0.30; – – –, 0.25. (b) $m = 3$: ——, $h(0) = 0.53$; — —, 0.50; · · ·, 0.45; – – –, 0.40. (c) $m = 10$: ——, $h(0) = 0.73$; · · ·, 0.70; – – –, 0.65.

than the minimum value in (52) a single large recirculating zone stretches between the two jumps. Lastly, the separating streamline for the recirculating regions is given for a power-law fluid by

$$h(0) = n_s - \frac{m+2}{m+1}\,\mathrm{sgn}\,(\sin\theta)\,|\sin^m\theta|\,h^{m+2}\left[\frac{m+1}{m+2} - \left(1-\frac{n_s}{h}\right) + \frac{1}{m+2}\left(1-\frac{n_s}{h}\right)^{m+2}\right].$$

2.5. *Partial films – power-law fluids*

For a film of limited extent, the equation for $h(\theta)$ becomes

$$q = h - h^{m+2}\,\mathrm{sgn}\,(\sin\theta)\,|\sin^m\theta| = 0. \tag{53}$$

Consequently, a positive, real solution for h exists for $0 \leqslant \theta \leqslant \pi$ and is given by

$$h = \left(\frac{1}{\sin\theta}\right)^{m/(m+1)}. \tag{54}$$

Once again, the term $\delta \mathrm{d}h/\mathrm{d}\theta$ in (43) must be reinstated in order to satisfy $h = 0$ at the film edges. Consequently, we must consider

$$q = h - h^{m+2}\left[\sin\theta + \delta\cos\theta\frac{\mathrm{d}h}{\mathrm{d}\theta}\right]^m = 0,$$

giving

$$\delta\cos\theta h^{1+1/m}\frac{\mathrm{d}h}{\mathrm{d}\theta} + \sin\theta h^{1+1/m} = 1. \tag{55}$$

Assuming that the film vanishes at $\theta = \theta_0$ and introducing $X = (\theta - \theta_0)/\delta$ in (55) we find

$$X = \frac{\cos\theta_0}{\sin\theta_0}\left\{-h + \int_0^h \frac{\mathrm{d}h}{1 - \sin\theta_0 h^{1+1/m}}\right\}. \tag{56}$$

As we approach the contact line, i.e. $X \to 0$, we have

$$h \propto X^{m/(2m+1)}, \quad \frac{\mathrm{d}h}{\mathrm{d}X} \propto X^{-(m+1)/(2m+1)},$$

and therefore as m increases, h vanishes more quickly and the film is not as blunt.

The remaining results analogous to those found for a Newtonian fluid are the results for small and large rotation rates. For small rotation rates Ω and therefore $\Gamma \gg 1$, we now have

$$q = h^{m+2}\left[\sin\theta + \delta\cos\theta\frac{\mathrm{d}h}{\mathrm{d}\theta}\right]^m + O\left(\frac{1}{\Gamma^m}\right) = 0. \tag{57}$$

The leading-order solution to (57) corresponds to a static film and naturally is independent of m and therefore identical with (36) found for a Newtonian fluid. When Ω is large, the rimming-flow solution analogous to (38) is

$$h = h(0) + \frac{\Gamma^m}{m+2}h(0)^{m+2}\,\mathrm{sgn}\,(\sin\theta)\,|\sin^m\theta| + O(\Gamma^{2m}). \tag{58}$$

3. Discussion

One important question remains, namely, under what conditions do the various steady-state film configurations occur? This question seems particularly interesting since the occurrence of continuous films that have sudden transitions or partial films on the rising side of the cylinder seem contrary to one's intuition. Unfortunately, the present work does not put us in a position to answer this question. In fact the answer surely requires investigating film stability and the initial-value problem (both of which are presently being pursued). However, a few comments and some speculation seem appropriate at this point.

The first comment regards the fact that there are limitations on the fluid volume for the various film configurations. For a gently varying continuous film (e.g. figure 1*c*) recall that we found that such a film configuration was possible provided

$$h(0) \leqslant \frac{m+1}{(m+2)^{(m+2)/(m+1)}}.$$

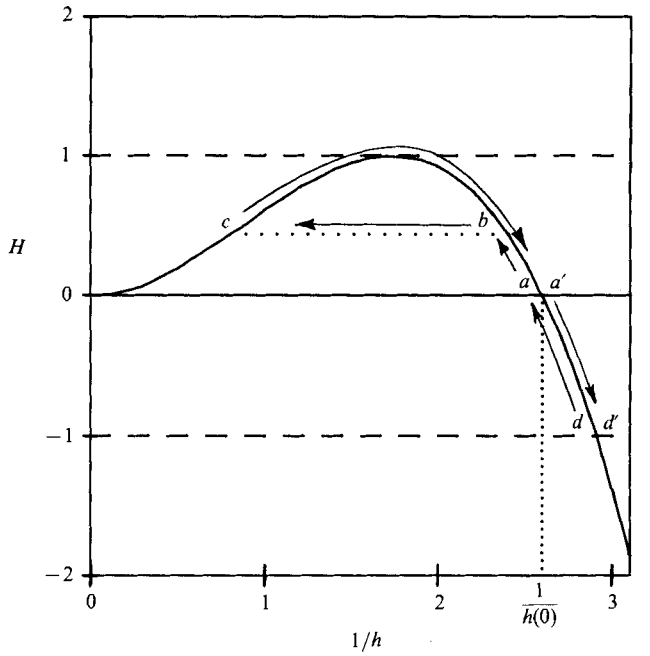

FIGURE 10. Locus of points $h(\theta)$ which describe a film having a single rapid transition ($h(0) = (m+1)/(m+2)^{(m+2)/(m+1)}$; see text for discussion).

This limitation naturally translates into a restriction on the film volume. For example, for $m = 1$ a gently varying continuous film is possible for $h(0) \leqslant 0.3849$ and therefore the film volume,

$$V = \delta R^2 \int_0^{2\pi} h(\theta)\,\mathrm{d}\theta,$$

must be less than or equal to $2.56\delta R^2$ (where $\delta = [3\mu\Omega/\rho g R]^{\frac{1}{2}}$ and the value 2.56 is the integral of $h(\theta)$ when $h(0) = 0.3849$). Consequently, gently varying continuous films might be the steady-state shape for fluid volumes less than this maximum. However, what configuration would occur for films having a greater volume than this maximum? Are continuous films with sudden transitions possible for greater volumes?

Consider the following thought experiment. Suppose that into a rotating cylinder we are slowly adding fluid in increments so that the film reaches a steady state for each volume increment. If each of these steady states corresponds to a gently varying continuous film then when the film volume first reaches its maximum value (corresponding to the maximum value of $h(0)$) perhaps a film having a sudden transition is born with the transition initially located near $\theta = \frac{1}{2}\pi$. As the volume is increased further the transition point would move upstream towards $\theta = 0$, but $h(0)$ might remain unchanged. A film profile of this type is described by the path of the arrows shown in figure 10. This case is possible when $h(0)$ is equal to its maximum possible value, in which case $H_{\max} = 1$. Here the film has a single rapid increase in depth (from point b to c) somewhere between $\theta = 0$ and $\frac{1}{2}\pi$. The film gradually increases in depth from $\theta = 0$ at a until it reaches the sudden transition at b. After the transition the film thins steadily and gradually (from c to a' to d') until $\theta = \frac{3}{2}\pi$ at which point it begins to thicken and return to $h(0)$ at $\theta = 2\pi$. Two typical examples

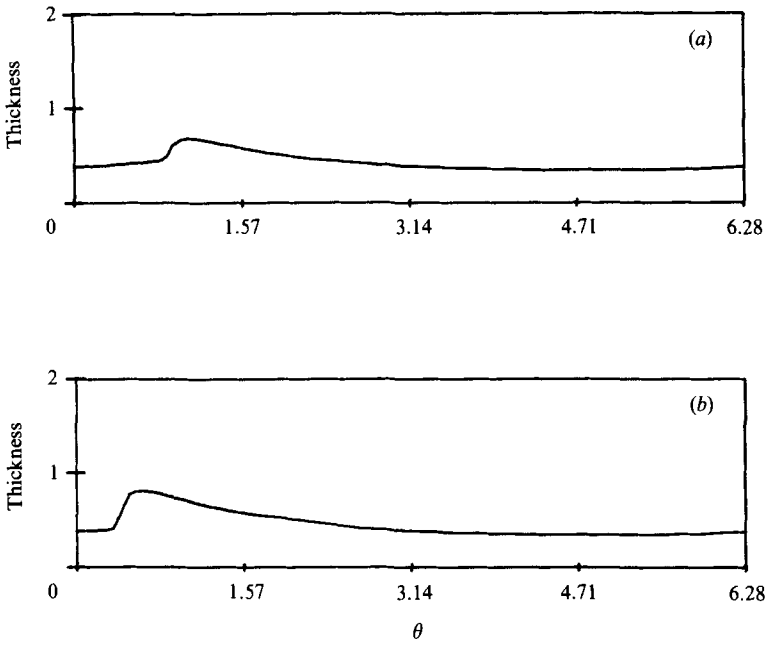

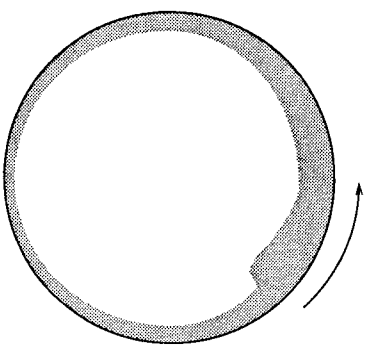

FIGURE 11. Typical film profiles of a film having a single transition and $m = 1$ ($h(0) = 0.3849$): (*a*) $\theta^* = 0.94$; (*b*) 0.44.

of such a film profile are shown in figure 11. Note also that the profile just described is very reminiscent of the cascading phenomena observed in the experiments conducted by White (1956), White & Higgins (1958) and Deiber & Cerro (1976), including the presence of recirculating zones, which have already been discussed. In addition, from a breakdown in their numerical calculations, Deiber & Cerro identified a region in which they believed discontinuous or sudden-transition solutions existed. However, their numerical scheme did not allow them to do computations in this region and they were forced to speculate about the character of these solutions. It is believed that the present transition solutions are of the class that Deiber & Cerro suspected were present.

Returning now to the thought experiment discussed above, as the film volume is increased, ultimately a maximum film volume is attained for this configuration when the transition point reaches $\theta = 0$. For $m = 1$, this maximum volume is found to equal $3.93\delta R^2$. Note that as the transition point approaches $\theta = 0$ the film thickness is unbounded, but integrable and so a finite maximum volume is predicted (this is easily verified by considering the solutions to (22) for θ near 0). However, what would occur for even greater volumes? Perhaps larger film volumes cannot be supported by the drag on the cylinder wall and only a large slightly perturbed puddle at the bottom of the cylinder can occur. Clearly the above thought experiment is pure speculation, but it is nonetheless amusing to consider the possibilities from the configurations that we have identified.

Note that other possibilities exist that are equally good candidates for explaining what happens when the fluid volume exceeds $2.56\delta R^2$ (the maximum volume for a gradually varied continuous film). One alternative to what was just described would be to have two transition points which would initially be near $\theta = \frac{1}{2}\pi$ and symmetrically located (examples of film configurations of this type have already been shown, see figure 7). Increasing the volume might move the two transition points towards $\theta = 0$ and $\theta = \pi$, but $h(0)$ would again remain fixed at its previous maximum ($h(0) = 0.3849$ when $m = 1$). Ultimately a maximum film volume for this configuration would also be attained when the transition points reach $\theta = 0$ and π. For $m = 1$ and $h(0) = 0.3849$ we find that this limiting volume is equal to $5.3\delta R^2$.

Now consider partial films trapped on the rising side of the rotating cylinder (e.g. figure 1*b*). For these cases we also find a maximum possible volume which occurs when the partial film extends from $\theta = 0$ to π. For $m = 1$ this maximum volume is easily shown to be $5.24\delta R^2$. Films of this type might be formed by injecting the fluid on the rising side of the cylinder at say $\theta = \frac{1}{2}\pi$ during rotation. Note, however, that partial films of this type and continuous films are both possible for a mutual range of volumes (e.g. for $m = 1$ partial films and gradually varied continuous films coexist as possible solutions for volumes $\leqslant 2.56\delta R^2$). Therefore the occurrence of one film configuration or another cannot be deduced from volume arguments alone. Nonetheless, considering the film volume suggests a number of possibilities and in some cases rules out the occurrence of some configurations. For example, for volumes greater than $2.56\delta R^2$ it is clear that a gradually varied continuous film is not possible.

It is also worth mentioning that there are other possible film configurations somewhat different from those already discussed which have interesting features of their own. For example, consider the film profile $h(\theta)$ generated by the path shown by the arrows in figure 12. Here the film steadily thickens as θ increases (proceeding from a to b) and becomes unbounded as θ approaches π at point b. This may describe the tendency of the fluid to drip from the top of the cylinder if the fluid volume is increased any further, in which case the rotating cylinder is unable to support the film and we have the onset of cascading or dripping. Although the physical interpretation for the unbounded film thickness at $\theta = \pi$ may be a little far-fetched, without some kind of explanation for this situation, one would generally discard this film configuration as a possible steady-state shape.

In conclusion, we found a number of interesting and amusing film configurations and have for the first time precisely identified transition film solutions. The obvious future direction is to determine when the various cases can occur. We have certainly not attempted to explore all of the possible cases in detail, but we have simply attempted to illustrate some of the possibilities. At this point there is probably little

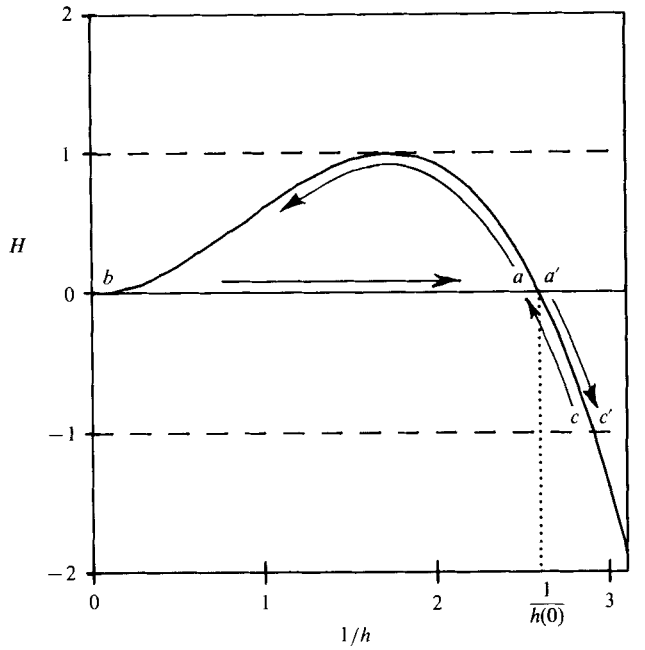

FIGURE 12. Locus of points $h(\theta)$ describing a gradually varying film which has $h(0)$ equal to its maximum value and becomes unbounded at $\theta = \pi$ (see text for discussion).

practical value in exploring any particular case thoroughly until it can be determined when, if at all, such a configuration occurs. The experiments by White & Higgins (1958) and White (1956) provide a good starting point for future work. Those experiments indicate that, for a fixed volume, a puddle exists at low rotation rates. As the rotation rate is increased the film exhibits cascading behaviour (similar to figure 11) and at still higher rotation rates eventually the film becomes a gradually varied continuous film or rimming film. Our own experiments have verified these general features. From the present work and the multiplicity of solutions found it is not too surprising that the film also displays interesting hysteresis behaviour as the rotation rate is subsequently changed.

This work was supported, in part, by a grant from the National Science Foundation (MSM 85-13795). I would like to thank R. P. Smet, Quan Qi and the referees for their useful comments.

REFERENCES

BALMER, R. T. 1970 The hygrocyst – a stability phenomenon in continuum mechanics. *Nature* **227**, 600–601.

DAVIS, S. H. 1983 Contact-line problems in fluid mechanics. *Trans. ASME* E: *J. Appl. Mech.* **105**, 977–982.

DEBLER, W. R. & YIH, C. S. 1962 Formation of rings in a liquid film attached to the inside of a rotating cylinder. *J. Aero. Sci.* **29**, 364.

DEIBER, J. A. & CERRO, R. L. 1976 Viscous flow with a free surface inside a horizontal rotating drum. I. Hydrodynamics. *Ind. Engng Chem. Fundam.* **15**, 102–110.

KARWEIT, J. J. & CORSSIN, S. 1975 Observation of cellular patterns in a partly filled, horizontal, rotating cylinder. *Phys. Fluids* **18**, 111–112.

ORR, F. M. & SCRIVEN, L. E. 1978 Rimming flow: numerical simulation of steady, viscous, free-surface flow with surface tension. *J. Fluid Mech.* **84**, 145–165.

PHILLIPS, O. M. 1960 Centrifugal waves. *J. Fluid Mech.* **7**, 340–352.

RUSCHAK, K. J. 1985 Coating flows. *Ann. Rev. Fluid Mech.* **17**, 65–89.

RUSCHAK, K. J. & SCRIVEN, L. E. 1976 Rimming flow of liquid in a rotating horizontal cylinder. *J. Fluid Mech.* **76**, 113–125.

TUCK, E. O. 1983 Continuous coating with gravity and jet stripping. *Phys. Fluids* **26**, 2352–2358.

VAN ROSSUM, J. J. 1958 Viscous lifting and drainage of liquids. *Appl. Sci. Res.* **A7**, 121–144.

WHITE, R. E. 1956 Residual condensate, condensate behavior, and siphoning in paper driers. *Tech. Assoc. Pulp Paper Ind.* **39**, 228–233.

WHITE, R. E. & HIGGINS, T. W. 1958 Effect of fluid properties on condensate behavior. *Tech. Assoc. Pulp Paper Ind.* **41**, 71–76.